Downloaded from rnajournal.cshlp.org on February 12, 2009 - Published by Cold Spring Harbor Laboratory Press

The 3′ proximal translational enhancer of Turnip crinkle virus binds to 60S ribosomal subunits

Vera A. Stupina, Arturas Meskauskas, John C. McCormack, et al.

RNA 2008 14: 2379-2393 originally published online September 29, 2008
Access the most recent version at doi:10.1261/rna.1227808

References This article cites 64 articles, 27 of which can be accessed free at:
http://rnajournal.cshlp.org/content/14/11/2379.full.html#ref-list-1

Article cited in:
http://rnajournal.cshlp.org/content/14/11/2379.full.html#related-urls

Open Access Freely available online through the open access option.

Email alerting service Receive free email alerts when new articles cite this article - sign up in the box at the top right corner of the article or **click here**

To subscribe to *RNA* go to:
http://rnajournal.cshlp.org/subscriptions

Copyright © 2008 RNA Society

Downloaded from rnajournal.cshlp.org on February 12, 2009 - Published by Cold Spring Harbor Laboratory Press

The 3′ proximal translational enhancer of Turnip crinkle virus binds to 60S ribosomal subunits

VERA A. STUPINA,[1,3] ARTURAS MESKAUSKAS,[1,3] JOHN C. MCCORMACK,[1] YAROSLAVA G. YINGLING,[2] BRUCE A. SHAPIRO,[2] JONATHAN D. DINMAN,[1] and ANNE E. SIMON[1]

[1]Department of Cell Biology and Molecular Genetics, University of Maryland College Park, College Park, Maryland 20742, USA
[2]Center for Cancer Research Nanobiology Program, National Cancer Institute, Frederick, Maryland 21702, USA

ABSTRACT

During cap-dependent translation of eukaryotic mRNAs, initiation factors interact with the 5′ cap to attract ribosomes. When animal viruses translate in a cap-independent fashion, ribosomes assemble upstream of initiation codons at internal ribosome entry sites (IRES). In contrast, many plant viral genomes do not contain 5′ ends with substantial IRES activity but instead have 3′ translational enhancers that function by an unknown mechanism. A 393-nucleotide (nt) region that includes the entire 3′ UTR of the Turnip crinkle virus (TCV) synergistically enhances translation of a reporter gene when associated with the TCV 5′ UTR. The major enhancer activity was mapped to an internal region of ~140 nt that partially overlaps with a 100-nt structural domain previously predicted to adopt a form with some resemblance to a tRNA, according to a recent study by J.C. McCormack and colleagues. The T-shaped structure binds to 80S ribosomes and 60S ribosomal subunits, and binding is more efficient in the absence of surrounding sequences and in the presence of a pseudoknot that mimics the tRNA-acceptor stem. Untranslated TCV satellite RNA satC, which contains the TCV 3′ end and 6-nt differences in the region corresponding to the T-shaped element, does not detectably bind to 80S ribosomes and is not predicted to form a comparable structure. Binding of the TCV T-shaped element by 80S ribosomes was unaffected by salt-washing, reduced in the presence of AcPhe-tRNA, which binds to the P-site, and enhanced binding of Phe-tRNA to the ribosome A site. Mutations that reduced translation in vivo had similar effects on ribosome binding in vitro. This strong correlation suggests that ribosome entry in the 3′ UTR is a key function of the 3′ translational enhancer of TCV and that the T-shaped element contains some tRNA-like properties.

Keywords: cap-independent translation; internal ribosome entry site; Turnip crinkle virus; translational enhancer

INTRODUCTION

Translating RNA sequences into functional proteins is a central activity for all organisms. While the elongation phase of translation (e.g., the peptidyltransferase reaction) is virtually identical across kingdoms, translation initiation varies widely and is intimately connected with kingdom-specific avenues of gene expression (Kozak 1999). Translation initiation in eukaryotic mRNAs requires that the template assume a closed loop structure, mediated by eukaryotic initiation factor eIF4E binding to the 5′ cap and poly(A)-binding protein binding to the poly(A) tail (Wells et al. 1998). Since both translation factors bind to the scaffold protein eIF4G, a bridge is formed between the 5′ and 3′ ends. eIF4G and associated proteins, known as eIF4F, recruit the 40S small ribosomal subunit and associated ternary complex (eIF2-GTP/Met-tRNA$_i$) to the cap region of the mRNA. The complex then "scans" in a 5′ → 3′ direction to the initiation codon, followed by release of some initiation factors, cleavage of GTP, and recruitment of the large 60S subunit to form the 80S ribosome followed by translation initiation (Preiss and Hentze 2003; Merrick 2004).

Many plant and animal viral RNAs have no 5′ cap, and ~3% of animal mRNAs also can use cap-independent mechanisms for translation under conditions when cap-dependent translation is impaired (Hellen and Sarnow 2001; Merrick 2004; Holcik and Sonenberg 2005). Animal plus-strand RNA viruses that lack 5′ caps contain large, internal ribosome entry sequences (IRES) that are located either in extensive (300–1500 nucleotides [nt]) 5′ UTRs or upstream of internal open reading frames (ORFs), and use different mechanisms to attract ribosomes (Hellen and Sarnow 2001). For example, Encephalomyocarditis virus (EMCV) IRES (~600 nt) interacts with canonical initiation

[3]These authors contributed equally to this work.

Reprint requests to: Anne E. Simon, Department of Cell Biology and Molecular Genetics, University of Maryland College Park, College Park, MD 20742, USA; e-mail: simona@umd.edu; fax: (301) 805-1318.

Article published online ahead of print. Article and publication date are at http://www.rnajournal.org/cgi/doi/10.1261/rna.1227808.

Downloaded from rnajournal.cshlp.org on February 12, 2009 - Published by Cold Spring Harbor Laboratory Press

factors to recruit the 40S ribosomal subunit, whereas the Hepatitis C virus (HCV) IRES (~360 nt) directly binds 40S subunits in the absence of eIFs and the ternary complex (Lancaster et al. 2006; Fraser and Doudna 2007). Dicistrovirus IRESs are unusual in that they can assemble 80S ribosomes without any eIFs and a portion directly serves as the initiator tRNA (Hellen and Sarnow 2001). Efficient translation using viral IRESs may also require sequences in the 3′ UTR of unknown function (Bradrick et al. 2006; Song et al. 2006), as well as host proteins (Baird et al. 2006) and/or additional viral-encoded proteins (Dobrikova et al. 2006).

Less than 20% of plant plus-strand RNA viruses have 5′ and 3′ ends that terminate with both 5′ caps and 3′ poly(A) tails (Dreher and Miller 2006). tRNA-like structures (TLS) with aminoacylated 3′ ends are found at the 3′ termini of many plant viruses in genera whose members also contain 5′ caps (Fechter et al. 2001; Dreher and Miller 2006). A proposal has been made that the TLS of Turnip yellow mosaic virus (TYMV) functionally replaces met-tRNA$_i$ during translation of a viral cistron, resulting in (or promoting) incorporation of the TLS amino acid at the N terminus of the viral polyprotein (Barends et al. 2003). However, other studies are contradictory with translation of both 5′ proximal TYMV ORFs, which are extensively overlapping, dependent on canonical cap-dependent recruitment of ribosomes that then scan to the closely spaced initiation codons, which compete for translation initiation (Matsuda and Dreher 2006).

Cap-independent translation of many plant viruses differs from that of animal viruses by involving elements in their 3′ UTR that enhance translation through unknown mechanisms (Fabian and White 2004; Shen and Miller 2004; Karetnikov et al. 2006; Miller et al. 2007). Such elements can bind to specific translation factors and either encompass or are associated with nearby sequence that form an RNA–RNA bridge with single-stranded complementary sequences near the 5′ end (Fabian and White 2006; Miller and White 2006).

Turnip crinkle virus (TCV), a member of the Carmovirus genus in the family *Tombusviridae*, contains a single 4054-nt plus-sense genomic RNA with five overlapping ORFs (Fig. 1A; Hacker et al. 1992). TCV is also associated with a dispensable subviral satellite RNA (satC) that is composed of a second satellite RNA and 151 bases derived from the TCV 3′ end (Simon and Howell 1986). TCV RNAs are not capped (Qu and Morris 2000) or polyadenylated, and the 3′ ends terminate with a hydroxyl group. The viral genomic and subgenomic RNAs are highly efficient templates for replication and/or translation, with viral

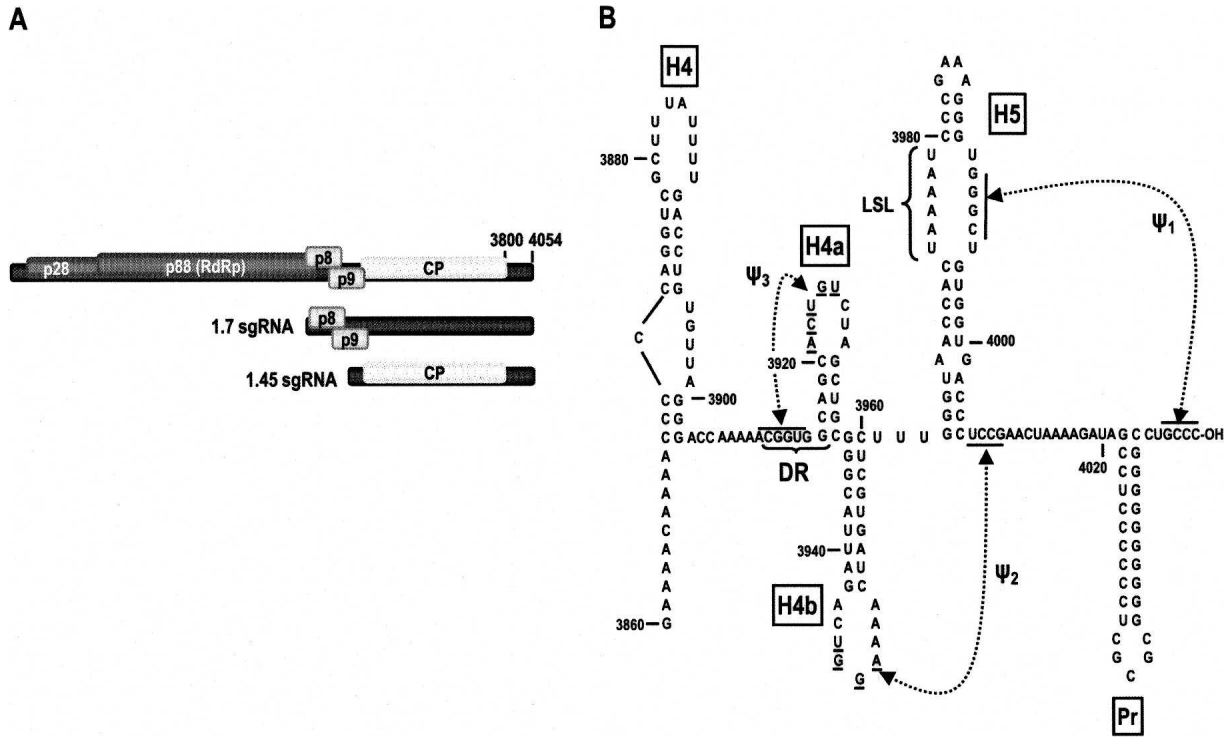

FIGURE 1. Genome organization and structure of the 3′ terminal region of TCV. (*A*) Genomic organization of TCV genomic and subgenomic RNAs. The RdRp (p88) is expressed as a ribosomal readthrough product of p28. The larger subgenomic RNA is the bi-cistronic mRNA for p8 and p9 movement proteins (Li et al. 1998), and the smaller subgenomic RNA encodes the viral capsid protein (Hacker et al. 1992). (*B*) Structure of the 3′ region of the TCV 3′ UTR. All secondary and tertiary structures have been previously confirmed using single and compensatory mutations (Zhang et al. 2006c; McCormack et al. 2008). (LSL) large symmetrical loop. Residues involved in pseudoknots are underlined or overlined. Names of the hairpins are boxed and pseudoknots designations are shown.

Downloaded from rnajournal.cshlp.org on February 12, 2009 - Published by Cold Spring Harbor Laboratory Press

RNAs reaching levels in cells comparable to ribosomal RNAs. The TCV 3′ UTR was reported to contain an unidentified element that synergistically enhances translation when present with the viral 5′ UTR (Qu and Morris 2000; Yoshii et al. 2004).

The TCV 3′ UTR contains five hairpins (from 5′ to 3′) (Fig. 1B): H4 along with flanking adenylates functions as a transcriptional enhancer in vitro (Sun and Simon 2006); H4a and adjacent H4b, which are required for viral accumulation in vivo (McCormack et al. 2008); H5, which is suggested to be an RdRp chaperone (McCormack and Simon 2004); and Pr, identified as a core promoter in the related subviral RNA satC (Song and Simon 1995). In addition to the hairpins, three pseudoknots have been identified (Zhang et al. 2006b; McCormack et al. 2008). H-type pseudoknot Ψ_3 connects the loop of H4a and upstream adjacent sequence known as the "DR" (de-repressor). The DR was previously identified as important for the satC conformational switch from its preactive to its transcriptionally active form (Zhang et al. 2006a,b). Ψ_2, originally identified in the preactive structure of satC (Zhang et al. 2006b), pairs sequence in the loop of H4b with residues adjacent to the 3′ side of H5, and Ψ_1, which links 3′ terminal residues with the 3′ side of the large symmetrical loop (LSL) of H5 (Zhang et al. 2006c). Subsets of elements from the related carmovirus *Cardamine chlorotic fleck virus* were able to functionally replace analogous TCV elements, suggesting that some elements interact to form at least three structural domains: H4 → 3′ end, Ψ_3 → H4b, and Ψ_3 → Ψ_2; the latter domain is predicted by the three-dimensional (3D) molecular modeling program RNA2D3D (Shapiro et al. 2007; Martinez et al. 2008) to fold into an internal T-shaped structure (TSS) (McCormack et al. 2008).

For this report, we mapped the major translational enhancer activity of TCV to an internal region of ~140 nt that overlaps with the TSS domain and determined that this domain independently binds to 80S ribosomes and 60S ribosomal subunits. Binding was unaffected by salt-washing, reduced in the presence of a canonical tRNA that binds the P-site, and not detected using the comparable region from untranslated satC. Mutations in the enhancer region that affect translation to various degrees had very similar effects on ribosome binding. The existence of 3′ ribosome-binding translational enhancers suggests that some viral and cellular mRNAs translated by cap-independent mechanisms with low 5′ UTR IRES activity (Bert et al. 2006; Nishimura et al. 2007) may be attracting ribosomal subunits through elements located in 3′ UTRs or coding sequences.

RESULTS

In vivo mapping of the TCV 3′ translational enhancer

Since translation-specific elements located in viral 3′ UTR may overlap with replication-specific sequences, an assay was used that separates the two processes. A reporter construct containing the firefly luciferase gene (FLuc) was engineered so that viral sequences could be added upstream and downstream of the reporter gene, and uncapped in vitro transcribed RNAs could be transfected into protoplasts and assayed for translation (Fig. 2A). As an internal control, RNA containing a different luciferase reporter (Rluc) was co-transfected, and all FLuc values were normalized to levels of Rluc.

RNA containing no added TCV sequence translated poorly (Fig. 2B). Addition of the complete TCV 5′ UTR upstream of the reporter gene (Fig. 2B, construct 5′ UTR) enhanced Fluc activity by 10-fold, suggesting that an element within the 5′ UTR enhances translation. Construct 5′UTR+3′C, which combined the 5′ TCV UTR with a control fragment from TCV minus strands (Fig. 2A, 3′C, positions 3393−3001) placed 3′ of the luc ORF did not significantly enhance activity over the 5′ UTR alone, suggesting that additional sequence at the 3′ end does not contribute to overall stabilization of the message. When the 3′ region from position 3661 to the 3′ end (FL) was added in the absence of 5′ viral sequences, a 21-fold enhancement of Fluc activity was achieved. When both 5′ and 3′ viral sequences were incorporated (Fig. 2B, 5′UTR+FL), translation was enhanced by 14-fold compared with 5′UTR+3′C (Fig. 2B). These results demonstrate a synergistic interaction between the TCV 5′ UTR and 3′ region, similar to what was previously reported (Qu and Morris 2000; Yoshii et al. 2004).

To determine more specifically the location of the 3′ translational enhancer, the Fluc construct containing the TCV 5′ UTR was altered to contain step-wise or internal deletions within the FL segment (Fig. 2C). When the 3′ segment contained sequence from 3661 to 3869, translational enhancement was only twofold above levels for 5′UTR+3′C (Fig. 2C). Extending the region to include partial (Fig. 2C, 3661–3895) or complete hairpin H4 (Fig. 2C, 3661–3911) either had no effect or slightly improved translation of Fluc. When the 3′ region also contained Ψ_3 and H4a, translational enhancement by the 3′ region increased to fourfold over 5′UTR+3′C levels. However, extending the 3′ region to include partial H4b sequence (Fig. 2C, through the terminal loop region; 3661–3951) caused a significant improvement in translation, with Fluc levels reaching 71% of levels achieved using the complete 3′ region, a 10-fold enhancement over 5′UTR+3′C levels. Further additions through H5 and Ψ_2 did not improve translational activity (Fig. 2C). These results suggest that the 5′ portion of the previously described Ψ_3 → Ψ_2 TSS domain (the Ψ_3–H4a region) is important for translation. Furthermore, achieving full (100%) enhancement by the 3661–4054 3′ segment requires the presence of sequence within the 3′ terminal 32 residues, suggesting an additional factor may exist in this region.

When the 5′UTR-Fluc construct contained the TCV 3′ terminus and upstream sequences extending partly into H4b

Downloaded from rnajournal.cshlp.org on February 12, 2009 - Published by Cold Spring Harbor Laboratory Press

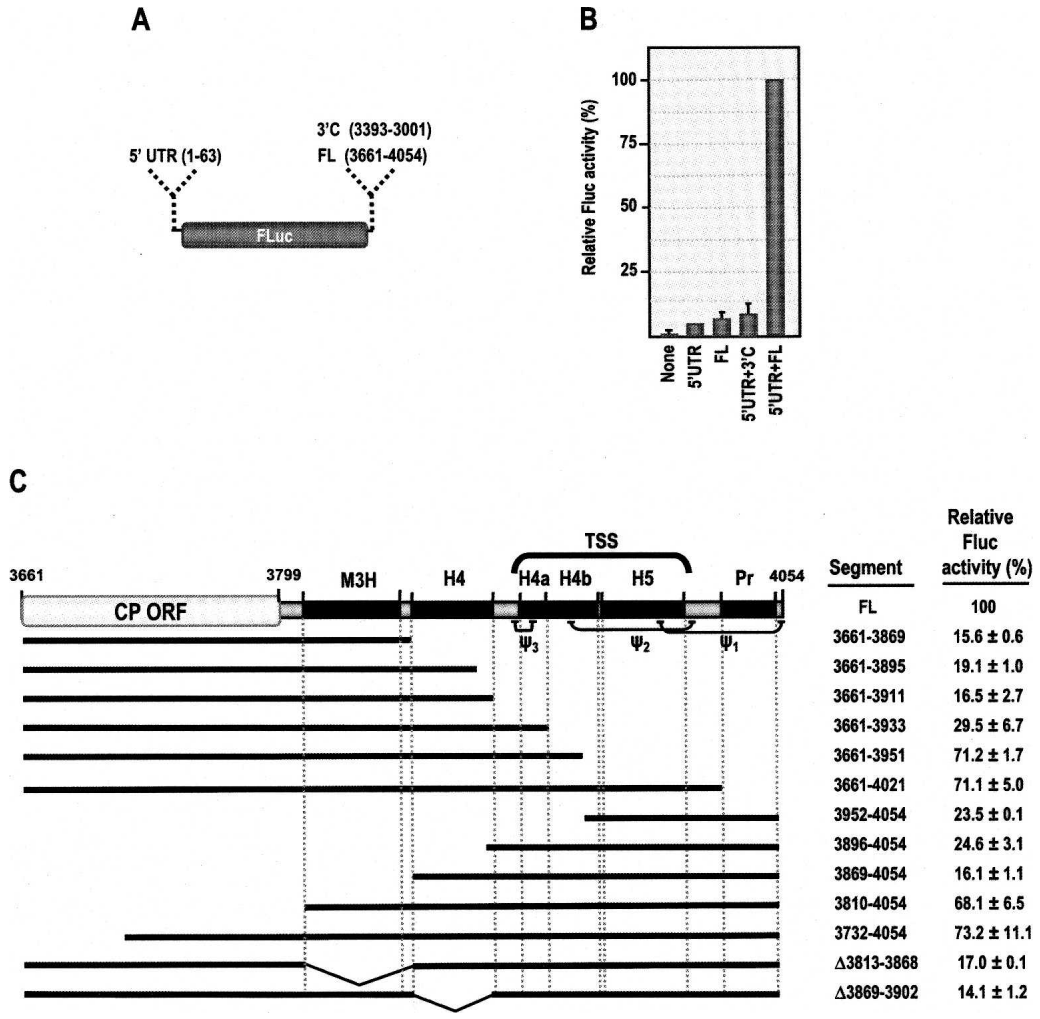

FIGURE 2. In vivo translation of a luciferase reporter construct in the presence and absence of viral 5′ and 3′ sequences. (*A*) Firefly luciferase reporter construct used for in vivo translation in protoplasts. The TCV 5′ UTR is 63 nt. The full-length TCV 3′ fragment (FL) includes the entire 3′ UTR and 139 nt from the CP ORF (positions 3661–4054). The 3′C control fragment is an internal segment of TCV (positions 3001–3393), inserted in the minus-sense orientation. (*B*) Relative translation in the presence and absence of the 5′ UTR and FL. *Arabidopsis* protoplasts were co-inoculated with 30 μg of RNA from experimental Fluc constructs and 10 μg of RNA synthesized from an internal control construct containing RLuc. Luciferase activity was determined at 18 hpi. All values are averages from at least three independent experiments, and standard deviation bars are shown. Transfected Fluc RNAs contained either no added TCV sequences (none), only the TCV 5′ UTR (5′UTR), only the 3′ region (FL), or both 5′ and 3′ sequences (5′ UTR+FL). (*C*) Effect of deletions within the FL fragment on translation from the 5′ UTR–Fluc construct. Fragments included in the constructs are denoted by a thick line. The positions of known TCV elements (hairpins and pseudoknots) and the TSS predicted to form from the $\Psi_3 \rightarrow \Psi_2$ domain (McCormack et al. 2008) are shown. Percent luciferase activity (averages of at least three independent experiments) with standard deviations is given.

(Fig. 2C, 3952–4054), translation was enhanced threefold over 5′UTR+3′C levels (Fig. 2C). Expanding this region to include sequence through Ψ_3 (Fig. 2C, 3896–4054) did not improve the efficiency of the region. A further extension to include the complete H4 hairpin reduced translational enhancement (Fig. 2C). These results suggest that the important Ψ_3–H4a region requires upstream sequences for function and that H4 has a negative effect on downstream sequences in the absence of upstream sequences. Extending the 3′ region an additional 59 bases (Fig. 2C, 3810–4054) improved translation to 68% of full enhancement levels, a ninefold increase over 5′UTR+3′C levels. Two deletion constructs were examined that remove elements that were previously found to be critical for TCV accumulation. Δ3813–3868 eliminated a region known as M3H; previous reports indicated that short deletions within this region abolished detectable TCV accumulation in protoplasts (Carpenter et al. 1995). Δ3869–3902 removed H4, which is also critical for TCV accumulation (Sun and Simon 2006). RNA containing either deletion was significantly worse as a template for translation, reducing levels of Fluc by six- to sevenfold. Altogether, these results indicate that full translational enhancement mediated by elements within the FL fragment (positions 3661–4054) was only achieved when

Downloaded from rnajournal.cshlp.org on February 12, 2009 - Published by Cold Spring Harbor Laboratory Press

the full fragment was used. In addition, these results suggest that the core region for translational enhancement extends from 3810 to 3951, which includes M3H, H4, and the Ψ_3–H4a portion of the previously identified TSS domain.

Mutations within H4 and Ψ_3 reduce translational enhancement mediated by the 3661–4054 fragment

To investigate the importance of specific structural elements within the 3810 to 3951 core translational enhancer region, mutations were generated in H4, Ψ_3, H5, and the linker region between H4 and Ψ_3 within the 5′ UTR-Fluc-FL construct (Fig. 3A). Mutations within the terminal and internal loops of H4, but not compensatory mutations in the stems, were previously determined to be detrimental for TCV accumulation in protoplasts (Sun and Simon 2006). Two new mutations that converted single uridylates to adenylates in the H4 terminal loop (Fig. 3A, m24,m39) reduced translation by moderate (40%) to high (threefold) levels (Fig. 3B). Alteration of multiple residues in the internal asymmetric H4 loop (Fig. 3A, m10,m21) caused sixfold reductions in translation, similar to the value obtained for deleting the entire hairpin (Fig. 2C). Altering five adenylates flanking H4 to uridylates (Fig. 3A, m49) also significantly affected translation, indicating that the influence of this region extends beyond the hairpin. To investigate whether the H4 uridylates in positions 3897 and 3898 pair with downstream adenylates, m10, which converts the two uridylates in the H4 asymmetric loop to adenylates, was combined with m49. Translation of m10+m49 was slightly worse than m10 alone, indicating that the combination was not compensatory (Fig. 3B). Previous investigation of a possible pseudoknot between uridylates on the 3′ side of the H4 terminal loop and these adenylates also did not support the existence of an interaction (Sun and Simon 2006).

To determine the importance of Ψ_3 for translational enhancement, single mutations in partner residues in the H4a loop (Fig. 3A, m27) and flanking sequence (Fig. 3A, m26) and the combined alterations that are compensatory for accumulation in vivo (McCormack et al. 2008) were generated in the 5′ UTR-Fluc-FL construct. m26 and m27 had identical threefold reductions in

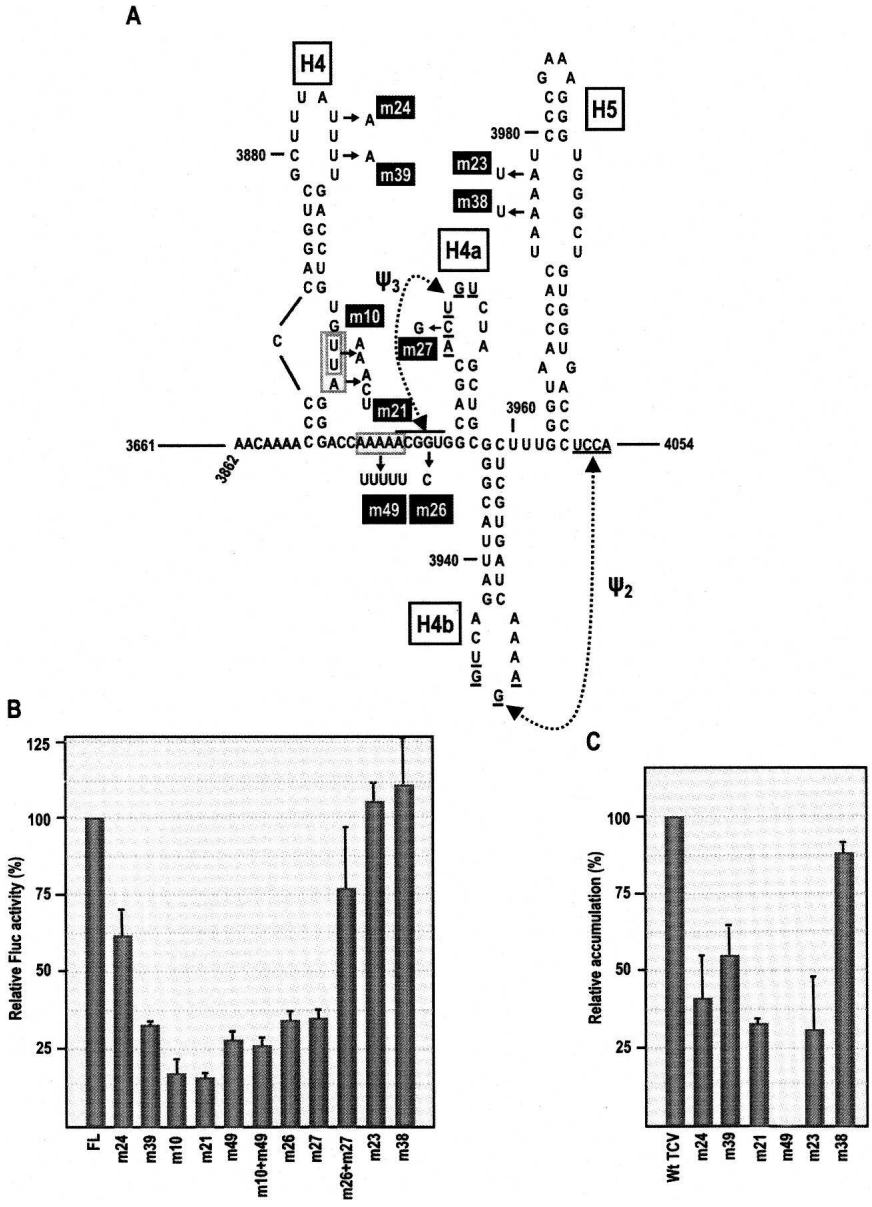

FIGURE 3. Mutations in H4 and Ψ_3 region repress translation in vivo. (*A*) Location of mutations generated in 5′UTR-Fluc-FL. Mutation designations are boxed. m10 replaces the consecutive two uridylates in the H4 asymmetric loop with adenylates; m21 replaces "UUA" in the same location with "ACU." (*B*) RNA transcribed from 5′UTR-Fluc-FL (FL) or 5′UTR-Fluc-FL containing mutations described in *A* along with RNA from the control Rluc construct were inoculated into protoplasts and luciferase activity measured at 18 hpi. Values are averages of at least three independent experiments. Bars reflect standard deviation. (*C*) Relative accumulation of TCV viral genomic RNA in protoplasts containing mutations in the 3′ region. Mutations were incorporated into full-length TCV cDNA and transcribed RNA inoculated into protoplasts. Viral RNA levels were determined by Northern analyses of total extracted RNA using a TCV-specific probe and normalized to the levels of ribosomal RNA. Values are from three independent assays. Bars reflect standard deviation. Accumulation of TCV containing m26, m27,m26+m27, and m10 were previously assayed (see text; Sun and Simon 2006; McCormack et al. 2008).

Downloaded from rnajournal.cshlp.org on February 12, 2009 - Published by Cold Spring Harbor Laboratory Press

Fluc levels in protoplasts while the mutations together restored translation to 77% of wild-type (wt) FL levels. In contrast, mutations in the adenylates within the large symmetrical internal loop of H5 (Fig. 3A, m23,m38), did not negatively affect translation.

The Ψ_3 mutations described above (Fig. 3A, m26,m27) had previously been assayed for effects on virus accumulation in protoplasts, an assay that reports on defects in both translation and replication. Both m26 and m27 reduced TCV to near undetectable levels, whereas the compensatory exchange improved accumulation to 55% of wt (McCormack et al. 2008). m10 also severely affected TCV levels, with accumulation reduced to 5% of wt (Sun and Simon 2006). To investigate the importance for virus accumulation of the other mutations evaluated in this study, full-length TCV genomic RNA was engineered to contain various mutations (Fig. 3A, m21,m23,m24,m38, m39,m49), and viral RNA accumulation assayed for in protoplasts. m24 and m39 in the loop of H4 reduced TCV accumulation to 41% and 55% of wt levels (Fig. 3C). m21 also reduced virus accumulation consistent with a negative role in translation, with mutant virus reaching 34% of wt levels. Altering the adenylates in the H4–H4a linker region (Fig. 3A, m49) eliminated detectable viral accumulation. The severity of the m49 mutations for viral accumulation compared to translation (3.5-fold reduction) likely reflects an additional role for the adenylates in replication (see Discussion). While mutations in the H5 LSL (Fig. 3A, m23,m38) did not affect translation, virus containing these mutations accumulated to 31% and 88% of wt levels, respectively, reflecting a role for some of the H5 LSL adenylates (e.g., A3978 [m23]) in replication (McCormack and Simon 2004; Zhang et al. 2006c).

$\Psi_3 \rightarrow \Psi_2$ TSS binds to 80S ribosomal subunits in vitro

It is currently not known how 3′ translational enhancers function in cap-independent translation. Molecular modeling of the $\Psi_3 \rightarrow \Psi_2$ region, which forms a functional domain based on substitution of elements with a related Carmovirus, suggested that this region folds into a structure that resembles a tRNA (TSS) (McCormack et al. 2008). When the TSS is superimposed on a canonical tRNA, the Ψ_3–H4a region is located in the "amino-acceptor" arm (see Fig. 6B, below). Since this region of a tRNA is known to be critical for interacting with ribosomes (Ulbrich et al. 1978), we assayed if TCV 3′ sequences could bind purified 80S yeast ribosomes in vitro using a filter binding assay. Yeast ribosomes could be used because of the high structural and functional conservation between eukaryotic ribosomes (Ganoza et al. 2002; Marintchev and Wagner 2004; Allen and Frank 2007). In addition, yeast ribosomes are very well characterized compared with plant ribosomes, have the ability to bind heterologous tRNAs (Ofengand et al. 1982), and have well-understood tRNA binding site specificity (Triana et al. 1994). Fragment FL (Fig. 4A, 3661–4054), the TSS alone (F1), $\Psi_3 \rightarrow$ 3′ end (F2), H4 $\rightarrow \Psi_2$ (F3), and H4 $\rightarrow$ 3′ end (F4) were subjected to the filter binding assays(Fig. 4). Of these fragments, ribosomes bound most tightly to F1 (K_d = 0.45 μM) and FL (K_d = 0.66 μM) (Fig. 4C). When H4 was included with the shorter fragments (F3, F4), binding was reduced by three- to fourfold. This suggested a negative effect of H4 on the structure of the shorter fragments that was reversed when additional upstream sequences were present (the FL fragment).

We next determined if ribosomes could bind to the Ψ_3–H4a region independent of most other sequences. Ribosome binding to F1 containing a full deletion of H5 (Fig. 4B, F1–ΔH5) was only twofold weaker than binding to F1 (Fig. 4B), while binding to a fragment containing only positions 3902–3951 (Fig. 4B, Ψ_3–H4a) was nearly fourfold weaker. These results suggest that ribosomes can bind to the Ψ_3–H4a region, but that the complete TSS allows for more optimal binding. To further examine the importance of the Ψ_3–H4a region for binding to F1, Ψ_3 mutations m26 or m27 were generated in F1. m26 and m27 each reduced ribosome binding to F1 by fivefold (Fig. 4C, F1-m26, F1-m27). Combining both mutations to reestablish the pseudoknot (Fig. 4C, F1-m26+m27) enhanced binding to near wt F1 levels (Fig. 4C), similar to the effect of the combined mutations on Fluc activity in vivo.

To determine if other mutations that reduce translational enhancer activity in vivo have a similar effect on ribosome binding in vitro, selected mutations that affect translation were incorporated into either the FL fragment (for mutations in the H4 region) or the F1 fragment. m10, located within the asymmetric loop of H4, reduced binding to the FL fragment by eightfold (Fig. 4C, FL-m10), similar to its sixfold reduction in translational enhancement. Mutating the adenylates flanking H4 to uridylates (Fig. 4C, FL-m49), which reduced translation by fourfold, reduced ribosome binding to the FL fragment by a similar amount. Altogether, these results strongly suggest that ribosome binding to at least a portion of the TSS affects translational enhancement by the 3′ region in vivo. In addition, H4 and flanking adenylates play an important role in translational enhancement in vivo and ribosome binding to FL in vitro.

A pseudoknot that forms between the terminal loop of H4 and the H5 LSL reduces ribosome binding in vitro

When H4 was included with the Ψ_3–H4a region, ribosome binding was not affected (Fig. 4C), suggesting that the negative effect of H4 on ribosome binding to F3 and F4 requires the presence of H5 (or Ψ_2). Examination of H4 and H5 revealed possible pairing between the H4 terminal loop (5′AUUUU) and the 5′ side of the H5 LSL (3′UAAAA) (denoted as Ψ_4 in Fig. 4B). To determine if formation of this potential kissing loop interaction was

Downloaded from rnajournal.cshlp.org on February 12, 2009 - Published by Cold Spring Harbor Laboratory Press

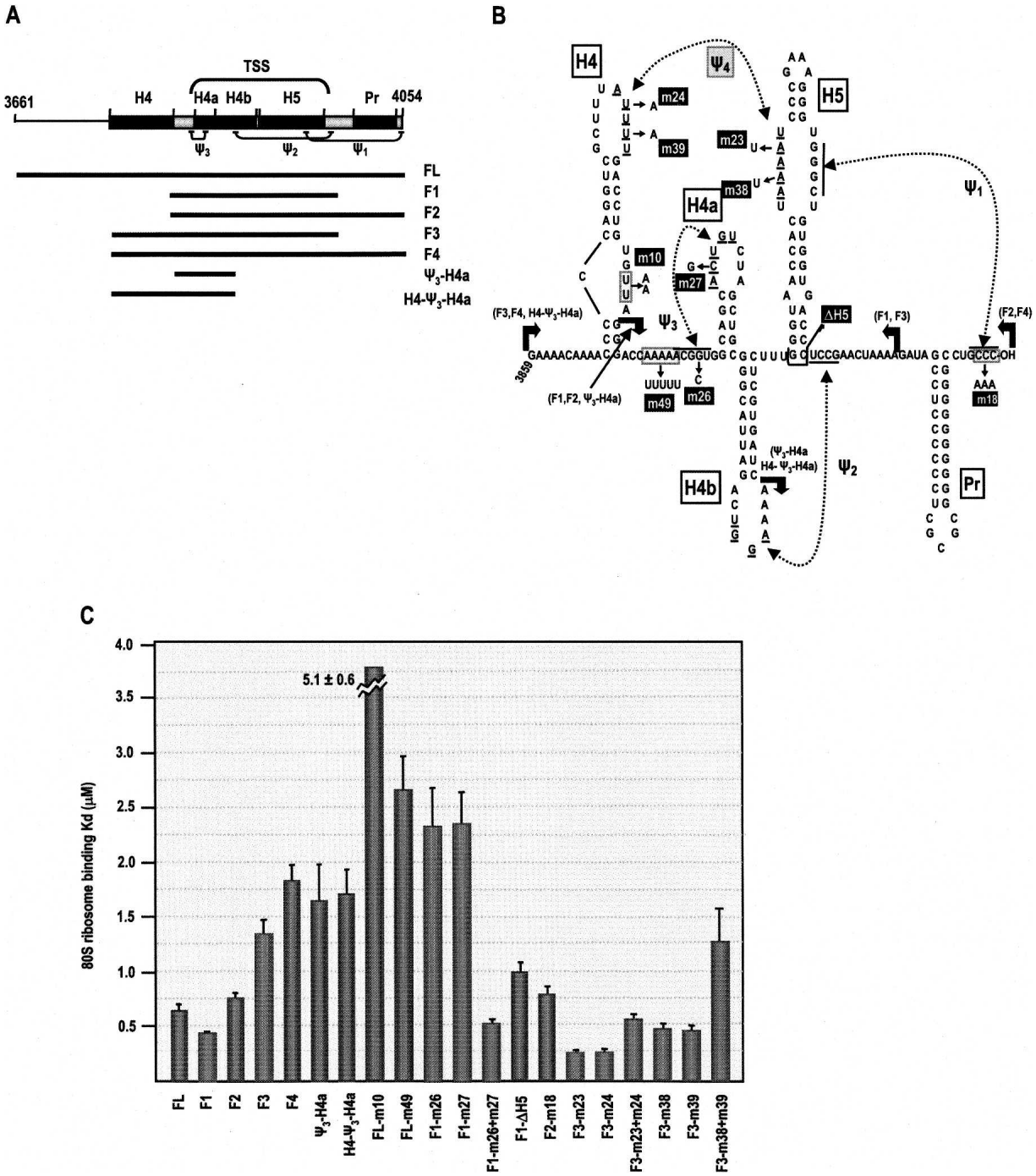

FIGURE 4. TCV 3′ sequences bind to yeast 80S ribosomes. (*A*) Location of fragments used for ribosome binding. Precise locations of the end points are indicated in *B*. Names of the fragments are given to the *right*. Location of 3′ elements is shown *above* fragments. (*B*) Mutations introduced into fragments are shown. Mutation designations are boxed. Thick bent arrows denote location of fragment end points, with identity of fragments using particular end points shown in parentheses. Ψ_4 forms between H4 and H5 in fragment F3 (see the text). (*C*) Wt and mutant fragments were subjected to filter binding assays using yeast 80S ribosomes. Columns 1–7 (*left* to *right*) are wt fragments. Remaining columns reflect fragments (FL, F1, F2, or F3) containing various mutations described in *B*. K_d were calculated from three independent experiments. Standard error bars are shown.

negatively impacting ribosome binding to short fragments containing the two hairpins (F3 and F4), two sets of single and compensatory exchanges were incorporated into the F3 fragment and mutant fragments assayed for ribosome binding. The presence of single mutations m23 (Fig. 4B, H5) and putative partner m24 (Fig. 4B, H4), identically enhanced ribosome binding to F3 by fivefold (K_d = 0.27 μM). The alterations together (Fig. 4B, m23+m24), which

Downloaded from rnajournal.cshlp.org on February 12, 2009 - Published by Cold Spring Harbor Laboratory Press

were predicted to restore Ψ_4, reduced ribosome binding by twofold (K_d = 0.58 μM, suggesting that an interaction inhibitory to ribosome binding was reestablished to some extent. m38 (Fig. 4B, H5) and m39 (Fig. 4B, H4) assayed in F3 also enhanced ribosome binding, reaching levels found in the absence of H4 (i.e., F1), whereas combining the mutations (Fig. 4B, m38+m39) reduced ribosome binding back to F3 levels (Fig. 4C). These results strongly suggest that a new pseudoknot forms between H4 and H5 when both hairpins are included in short fragments.

We also examined if reduced ribosome binding to F2 compared with F1 was a consequence of Ψ_1, which is present in F2 but not F1. We previously demonstrated that Ψ_1 exists in F4 (F2 was not assayed) by altering the 3′ end to prohibit pseudoknot formation and determining that the structure of the F4 fragment differs nearly exclusively in the H5 region (McCormack et al. 2008). The 3′ end mutations (Fig. 4B, CCC–AAA, m18), however, had no effect on ribosome binding to F2, indicating that reduced ribosome binding was not associated with the presence of Ψ_1.

F1 interaction with ribosomes is reduced by a tRNA that targets the P-site and occurs in the absence of translation factors

To determine if the binding site on 80S ribosomes overlaps canonical tRNA-binding sites (A, P, or E sites), bind and chase assays were performed using uncharged (nonacylated) $tRNA_{Phe}$ ($tRNA_{Phe}$), which binds to the P-site of nonprogrammed ribosomes, charged Phe-tRNA, which binds to P- and A-sites, and acetylated Phe-tRNA (Ac-Phe-tRNA), which is specific for the P-site (Wilson et al. 2000). Twenty-fold excess of uncharged tRNA reduced binding of nonprogrammed ribosomes to the preincubated F1 fragment by 61% (Fig. 5A), while the same amount of excess F1 reduced binding of acetylated Phe-tRNA to programmed ribosomes by 52% (Fig. 5B). Binding of the TCV element to 80S ribosomes significantly stimulated binding of Phe-tRNA to the A-site in the absence (Fig. 5B) of preincubation with tRNA to saturate the P-site. Addition of F1 to ribosomes where the P-site was blocked by addition of tRNA also did not compete with Phe-tRNA binding to the A-site (not shown). Altogether, these data indicate that the F1 binding site is in the vicinity of the 80S P-site.

Depending on the IRES element, ribosome interaction may be dependent or independent of additional translation factors (Hellen and Sarnow 2001; Baird et al. 2006; Fraser and Doudna 2007). To determine if binding to F1 occurs in the absence of translation factors, ribosomes were washed in buffer containing 0.5 M KCl during the isolation procedure to remove associated proteins. Salt-washed ribosomes bound to F1 with the identical K_d as ribosomes

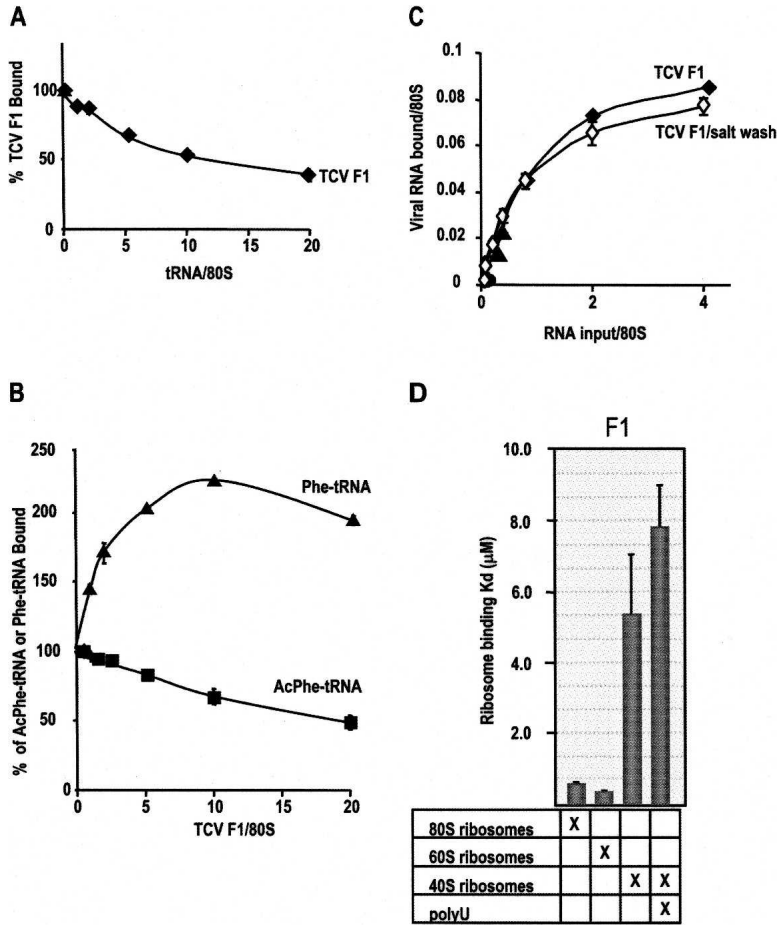

FIGURE 5. Features of ribosome binding to fragment F1. (*A*) Effect of deacylated tRNA on ribosome binding to F1. Ribosomes (30 pmol) were preincubated with 0–600 pmol of tRNA followed by addition of 30 pmol of [^{32}P] 5′-end labeled F1. (*B*) Effect of F1 on Phe-tRNA and Ac-Phe-tRNA binding. For P-site specificity, ribosomes (30 pmol) were incubated with 0–600 pmol of F1 followed by addition of 30 pmol of labeled Ac-Phe-tRNA. For A site competition, ribosomes were preincubated with 0–600 pmol of F1, followed by addition of labeled Phe-tRNA. Data are expressed as percentage of initial binding (without competing RNA) at given competing RNA/ribosomes molar ratios. (*C*) F1 binding to 80S ribosomes. Two to 100 pmol of labeled F1 were combined with 25 pmol of yeast 80S ribosomes that were and were not salt washed, and bound RNA was detected following filter binding. The fraction of ribosomes active in F1 binding is comparable with yeast Phe-tRNA binding with similarly prepared yeast ribosomes from the same yeast strain (Petrov et al. 2004). (*D*) Binding of 80S ribosomes and 60S and 40S ribosomal subunits to labeled F1 in the presence and absence of poly(U). For all assays, K_d were calculated from three independent experiments. Standard error bars are shown.

Downloaded from rnajournal.cshlp.org on February 12, 2009 - Published by Cold Spring Harbor Laboratory Press

isolated in the absence of salt, indicating that binding can occur in the absence of translation factors (Fig. 5C).

F1 binds to 60S ribosomal subunits

Although free 80S ribosomes can be more prevalent than 60S and 40S subunits under certain growth conditions, interaction of F1 with one of the ribosomal subunits is more likely. To test for F1 binding to ribosomal subunits in vitro, 80S ribosomes were dissociated and gradient fractionated 40S and 60S subunits were assayed for F1 binding (Fig. 5D). F1 bound to 60S subunits slightly better than to 80S ribosomes (K_d = 0.34 μM) whereas the affinity of F1 for 40S subunits was nearly 16-fold lower. In the presence of poly(U), which possibly blocks nonspecific F1/40S interactions in the mRNA channel, binding to 40S subunits was 23-fold lower than binding to 60S subunits. These results suggest that the low level 40S binding was partly nonspecific and that F1 interaction with 80S ribosomes is mainly through binding to the 60S subunit.

SatC does not form a comparable TSS and does not bind ribosomes in vitro

The satC 3′ terminal region was originally derived from two regions of TCV, including a fragment extending from the 3′ side of the H4 lower stem through the 3′ end (Simon and Howell 1986). Within the comparable sequence to F1, satC contains 6-nt differences: two in the Ψ_3–H4a region, one in H4b loop, one in the linker sequence between H4b and H5, and two in H5 (Fig. 6A). When the satC F1 equivalent fragment was assayed for ribosome binding, binding was reduced by 88-fold (K_d = 37 μM) (data not shown), suggesting that one or more of these nucleotide differences affects the ability of this satC region to serve as a ribosome-binding template.

To determine if the satC region corresponding to the TCV $\Psi_3 \rightarrow \Psi_2$ domain is predicted to assume a TSS, RNA2D3D along with molecular modeling (Yingling and Shapiro 2006; Shapiro et al. 2007; Martinez et al. 2008; McCormack et al. 2008) was used to predict the structure of this region of satC. Using the TCV TSS as a base structure, the 6-nt differences in satC were found to produce significant destabilizing effects, with both Ψ_2 and Ψ_3 losing their standard base-pairing interactions (Fig. 6B,C). SatC base differences in H5 were also predicted to increase the kink and flexibility of the helix. The apparent inability of satC to form a TCV-like structure in this region correlates with lack of detectable ribosome binding and is consistent with previous results demonstrating that satC Ψ_2 is present in a preactive structure that does not contain H5 (Zhang et al. 2006a). Additionally, we have recently determined that Ψ_3 does not form or is not important in satC (R. Guo and A.E. Simon, unpubl.). Since satC is not translated, the presence of a translational enhancer in the region is not required and thus sequences may have evolved to participate in different required functions.

DISCUSSION

Role of the 3′ internal TSS in translational enhancement

IRESs located within the 5′ UTR of cap-independently translated animal RNA viruses are extensive, highly structured elements that either directly bind to 80S ribosomes or 40S ribosomal subunits or associate with ribosomes through translation initiation factors or accessory proteins (Hellen and Sarnow 2001; Baird et al. 2006; Fraser and Doudna 2007). While several plant virus families also have 5′ IRES elements that contribute to cap-independent translation (Kneller et al. 2006), these elements tend to be more limited in size, with little sequence or structural conservation even within families. In addition to or in place of 5′ elements, many plant viruses have diverse translational enhancers in their 3′ UTR that also vary substantially in sequence and structure (Kneller et al. 2006; Miller et al. 2007). The best studied enhancer, the cap-independent translation element (CITE) associated with Barley yellow dwarf virus, binds to eIF4F through its eIF4G subunit, which may be delivered to the 5′ end through an RNA–RNA kissing loop that forms between hairpins in the 5′ and 3′ UTR (Miller and White 2006; Treder et al. 2008). Translational enhancers have also been found in 3′ UTR of animal viruses (Chiu et al. 2005; Bradrick et al. 2006; Song et al. 2006), with proposed functions in template circularization, translation termination, the switch between translation and replication, and ribosome recycling.

We previously determined that the 3′ UTR of TCV contains several functional modules, including one that contains three hairpins encompassed by two pseudoknots ($\Psi_3 \rightarrow \Psi_2$). This internal domain is predicted to adopt a TSS that somewhat resembles a tRNA according to a new molecular modeling protocol (McCormack et al. 2008). For this study, we mapped the TCV 3′ translational enhancer to an extended region that comprises a large fraction of the 3′ UTR, including a portion of the TSS (Fig. 2). Inclusion of the Ψ_3–H4a region with upstream sequences significantly improved translational enhancement, suggesting that this region contains one or more important components for TCV translation. The additional increase in translation when the partial H4b sequence is present with Ψ_3–H4a may reflect enhanced stability of the Ψ_3–H4a structure.

Compared with construct 5′UTR+3′C, which contains an internal TCV fragment 3′ of the reporter ORF, translation increased threefold when the 3′ fragment consisted only of sequence downstream of the Ψ_3–H4a region (Fig. 2, 3952–4054). Translational enhancement conferred by upstream 3′ sequences also increased when the 3′ terminal region was included. One possibility is that the 3′ terminal

Downloaded from rnajournal.cshlp.org on February 12, 2009 - Published by Cold Spring Harbor Laboratory Press

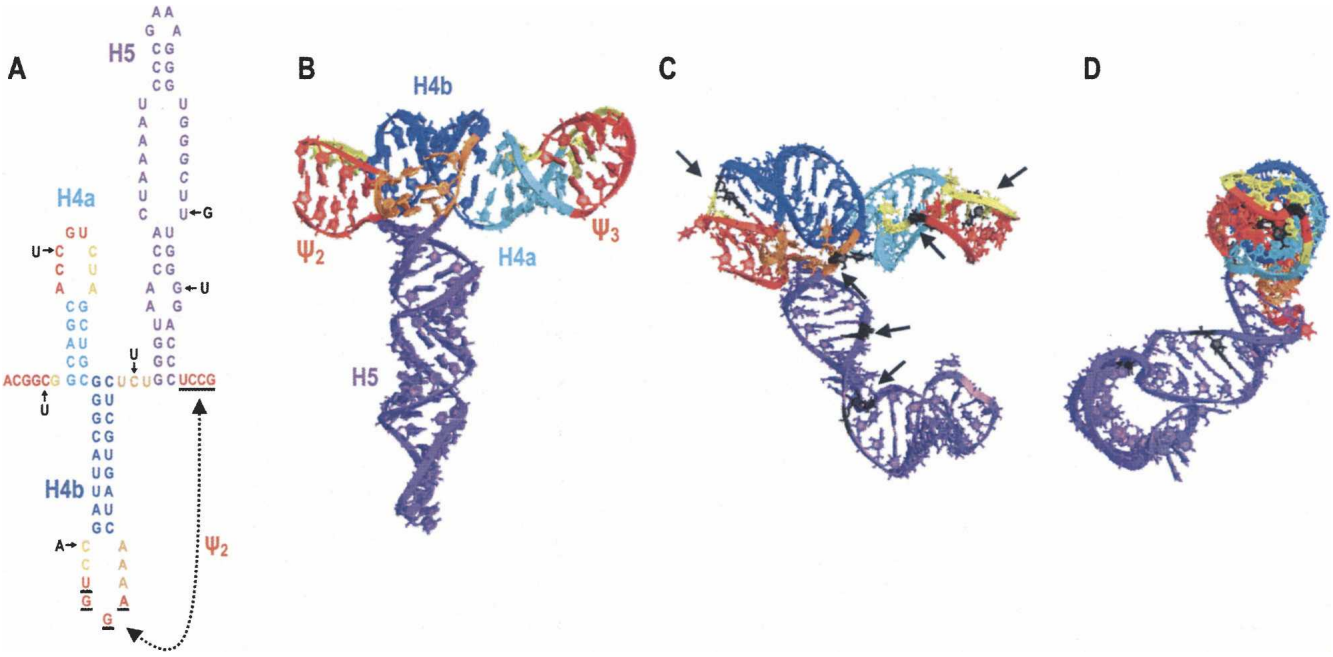

FIGURE 6. SatC structure predicted by RNA2D3D and molecular modeling. (*A*) SatC sequence in the region corresponding to the TCV $\Psi_3 \rightarrow \Psi_2$ domain. The 6-nt differences with the TCV sequence (in black) are shown. Color coding of sequences is used to help identify regions in the 3D structure shown in *B–D*. Underlined residues participate in Ψ_2 interaction in satC. Although presented with the hairpins in the figure, this pseudoknot does not coexist in the same satC structure as H5 (Zhang et al. 2006a). (*B*) TCV TSS predicted by RNA2D3D and molecular modeling (McCormack et al. 2008). (*C*) Predicted structure of the comparable region of satC. Arrows point to the locations in the structure occupied by the 6-nt differences. Note that Ψ_3 and Ψ_2 are not stably maintained. (*D*) Side view of the satC structure.

region serves as a poly(A) tail mimic that contributes to translation by a mechanism separate from the upstream element as described for Red clover necrotic mosaic virus and Tobacco necrosis virus (Iwakawa et al. 2007; Shen and Miller 2007). Interestingly, inclusion of sequences upstream of the Ψ_3–H4a region was required to further improve translation mediated by fragments containing the 3′ end. Deletion of M3H significantly affected translational enhancement by the 3′ region, suggesting that M3H may be required for synergy between the 5′ and 3′ ends when the 3′ end includes the Ψ_3–H4a region or may impact ribosome binding to the TSS in an unknown fashion. In its minus-sense orientation, M3H can enhance transcription from promoter elements in vitro and serves as an RNA recombination hot spot in vivo, which required maintenance of a large minus-sense hairpin within the region (Carpenter et al. 1995; Nagy et al. 1999). Deletions in several noncontiguous regions within and upstream of this segment eliminated detectable TCV accumulation in protoplasts (Carpenter et al. 1995). These results suggest that the M3H region plays an important, but as yet undefined, role in translation and replication.

Ribosome binding to the Ψ_3–H4a region correlates with translational enhancement

Based on modeling, the Ψ_3–H4a region in the TSS occupies a similar position as the amino-acceptor stem of a canonical tRNA (McCormack et al. 2008). Since this portion of a tRNA is directly involved in binding the ribosome peptidyltransferase center (Ulbrich et al. 1978), we questioned whether translational enhancement might involve interaction of the enhancer region with ribosomes. Both 80S ribosomes and 60S ribosomal subunits bound to the TSS, and binding was not improved by inclusion of upstream and/or downstream sequences (Fig. 4). The ribosome binding constant for fragment F1 was ~10-fold weaker than the binding constant of yeast aminoacylated-tRNA for yeast 80S ribosomes (K_d = 0.05 μM; Petrov et al. 2004) and comparable to binding of deacylated tRNA to *Escherichia coli* ribosomes (0.1–0.25 μM) (Schilling-Bartetzko et al. 1992). The lower affinity of F1 for ribosomes compared with canonical tRNAs may reflect the absence of codon/anticodon interactions to stabilize binding. Alternatively, molecular dynamics simulations (50 nsec with explicit solvent) predicted that the TSS varies significantly over time, with the H5 helix contracting in size and/or bending toward the 3′ end before returning to a form similar to the starting structure (McCormack et al. 2008; W. Kasprzak and B.A. Shapiro, unpubl.). If the simulation is accurate, then the K_d may be underestimating the efficiency of ribosome binding since the interaction may be limited to a subset of TSS conformations.

Bind and chase assays suggested specificity of the TCV element for the ribosome P-site (Fig. 5). The low chasing

Downloaded from rnajournal.cshlp.org on February 12, 2009 - Published by Cold Spring Harbor Laboratory Press

efficiency of tRNA possibly results from significantly lower affinity of tRNA for the P-site of nonprogrammed ribosomes (Rheinberger et al. 1981), additional binding of the F1 fragment to the E-site, or quality of the commercial preparation of tRNA. Additional evidence for at least partial occupation of the P-site by F1 comes from finding that preincubation of ribosomes with F1 stimulated binding of amino-acylated tRNA to the A-site. Enhanced binding of charged tRNAs to the A-site when the P-site is occupied by deacylated tRNA has been previously demonstrated (Van Noort et al. 1985).

Evidence that ribosome affinity for the 3′ region is related to translational enhancement came from finding that nearly all mutations tested had similar effects on Fluc activity in vivo and ribosome binding to either FL or F1 fragments in vitro (Figs. 3, 4). These mutations included ones that disrupted or reformed Ψ_3 (Fig. 3A, m26, m27,m26+m27; Fig. 4B, m26,m27,m26+m27), altered adenylates upstream of Ψ_3 (Figs. 3A, 4B, m49), or altered H4 (Figs. 3A, 4B, m10,m24,m39). m26 and m27 were previously found to reduce full-length TCV accumulation to >2% of wt in protoplasts, whereas restoring the pseudoknot returned TCV levels to 55% of wt (McCormack et al. 2008). m49 eliminated detectable TCV accumulation while reducing Fluc activity by only 3.5-fold. We have recently determined that mutating these adenylates suppresses specific RdRp binding to the 3′ region of the virus, which could account for the more severe effect of m49 on virus accumulation (M. Young and A. E. Simon, unpubl.). While the H5 mutations had no effect on translation and deletion of H5 only reduced F1 ribosome binding by twofold, previous mutations in H5 (McCormack and Simon 2004) and m23 (this report) significantly lowered TCV accumulation in protoplasts. We previously demonstrated that accumulation of nontranslated satC requires maintenance of H5 structure and the LSL adenylates (Zhang et al. 2004; Zhang and Simon 2005). H5 and the equivalent hairpin in tombusviruses (SL3) have been proposed to function as chaperones for assembly of the RdRp (McCormack and Simon 2004; Panaviene et al. 2005; Na and White 2006). Our recent determination that some LSL adenylates are required for one-site RdRp binding to the F4 fragment (M. Young and A.E. Simon, in prep.) further supports an important role for H5 in virus replication.

Role of H4 in translation

Deletion of H4 or alteration of the hairpin's asymmetric loop (m10 and m21) significantly reduced accumulation of TCV in protoplasts, translation of Fluc in protoplasts, and ribosome binding to the FL fragment in vitro (Figs. 3, 4; Sun and Simon 2006; McCormack et al. 2008). Alterations in the H4 terminal loop (Fig. 3A, m24,m39; Fig. 4B, m24,m39) also reduced translation and accumulation in vivo. The presence of H4 in fragment F3 reduced ribosome binding due to the formation of a new kissing loop interaction between the H4 terminal loop and the H5 LSL, as determined by two sets of compensatory alterations. However, there is no evidence that this pseudoknot is biologically relevant. m38, which disrupts the pseudoknot in F3, had no significant effect on translation of Fluc in vivo when incorporated into the larger FL fragment (Fig. 3B) and only slightly decreased virus accumulation when present in full-length TCV (Fig. 3C). One possibility is that the terminal loop of H4 naturally interacts with a sequence missing from F3, and that this interaction prevents an unidentified element from negatively impacting ribosome binding to the TSS. The possible artificial formation of Ψ_4 in truncated fragments containing H4 and the TSS could account for the lack of enhanced translation of Fluc when the 3′ segment contained the entire TSS (the preferred ribosome binding substrate) as opposed to terminating just past the Ψ_3–H4a region (Fig. 2).

Model for translational enhancement by 60S ribosome subunit entry at the 3′ end

A major question is how 60S subunits are transferred from the TSS to the 5′ end prior to initiation of translation. Since the second major arm of the TSS has no evident similarity to the tRNA anticodon domain and does not contain sequence that could serve as an methionyl anticodon, translation initiation in TCV is unlikely to resemble that of the dicistroviruses, where the IRES substitutes for the initiator tRNA by mimicking the interaction between anticodon and mRNA codon (Wilson et al. 2000; Costantino et al. 2008). Although other viruses in the *Tombusviridae* have 3′ elements that pair with complementary sequences in the 5′ UTR (Fabian and White 2004; Dreher and Miller 2006; Miller and White 2006; Miller et al. 2007), no obvious sequences complementary to single-stranded regions in the TSS or surrounding regions are discernable in the TCV 5′ UTR, with the exception of sequence complementary to the H4 loop. Mutations in this complementary sequence in the 5′ UTR, however, had only a limited effect on TCV accumulation in protoplasts, and compensatory mutations did not support such an interaction (V. Stupina, J.C. McCormack, and A.E. Simon, unpubl.). Furthermore, TCV accumulates to wt levels when its 5′ UTR is replaced with the 5′ UTR of *Japanese iris necrotic ring virus*, which has no discernable sequence similarity outside of five residues at the 5′ terminus (J.C. McCormack and A.E. Simon, unpubl.). Therefore, circularization of the template may not involve direct RNA:RNA interactions.

In one possible model (Fig. 7), the small ribosomal subunit (in association with the ternary complex) enters within the TCV 5′ UTR, scans to the initiation codon, and is then joined by the large subunit/3′TSS complex, leading to circularization of the template. Assembly of the 80S ribosome would require prior release of the TSS to correctly

Downloaded from rnajournal.cshlp.org on February 12, 2009 - Published by Cold Spring Harbor Laboratory Press

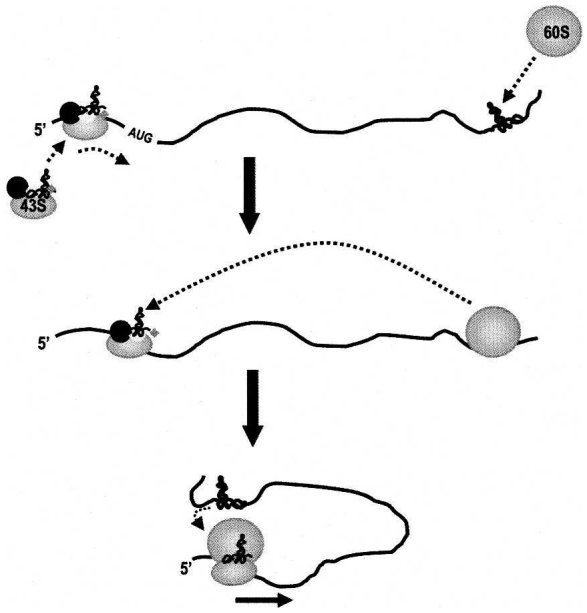

FIGURE 7. Model for translational enhancement by 3′ sequences in TCV. Our data suggest that the 5′ UTR and 3′ UTR work synergistically to mediate translation in TCV. We suggest that the large 60S ribosomal subunit binds to the TSS while the 43S preinitiation complex enters at the 5′ UTR. Circularization of the template could be mediated by assembly of the 80S ribosome, which would require that the 60S subunit release the TSS to position the initiator met-tRNA in the P-site. We propose that H4 (not shown) plays a critical role in translation, possibly by interfering with a ribosome-binding repressor. Such a repressor could become active following RdRp binding to the same region, to restrict ribosome binding and thus help mediate the switch between translation and replication. Additional upstream sequences are also important for translation, such as those in the M3H region, possibly to assist in ribosome relocation to the 5′ end.

position the initiator met-tRNA in the P-site. The lower affinity of ribosomes for the TSS as compared to aminoacylated-tRNA (e.g., initiator tRNA) would favor exchange of large subunits from the TSS to the 43S preinitiation complex. The TSS may also enhance translation by participating as a local sink for large ribosomal subunits following disassembly of the post-termination ribosomal complex allowing for more rapid ribosome reinitiation.

Ribosome entry near the 3′ end could provide a means for plus-strand viruses to precisely control timing of the switch from translation to replication of the initial infecting viral genomes. Ribosome binding to a region that also serves as a promoter for the RdRp could preclude premature binding of newly synthesized RdRp, allowing translation of the viral genome to continue until a threshold level of RdRp has been synthesized. We have recently determined that RdRp binding causes a substantial conformational shift in the Ψ_3–H4a region, upstream adenylates/H4, and in the lower stem and LSL of H5 (X. Yuan, M. Young, and A.E. Simon, unpubl.). Altering the conformation of the RNA in the region could suppress further ribosome binding by eliminating Ψ_3, allowing RdRp to reiteratively transcribe complementary strands.

The substantial conservation of eukaryotic ribosomes and translation factors suggests that translational enhancers in 3′ UTR that function in cap-independent translation in plants and animal viruses may have counterparts in other eukaryotes. Such 3′ elements may have been overlooked, since some (including the TCV 3′ region) are not responsive in traditional in vitro assays (Wu and White 1999; Song et al. 2006; V. Stupina and A.E. Simon, unpubl.) possibly due to the absence of required translation factors. Our discovery of a 3′ proximal element with 60S binding activity indicates that ribosome subunit entry/reentry may not be restricted to regions upstream of initiation codons and suggests that viral and cellular RNAs translated in a cap-independent fashion without strong 5′ IRES elements (Bert et al. 2006; Nishimura et al. 2007) may have additional unidentified translational enhancers that attract ribosomal subunits in 3′ UTR or coding sequences.

MATERIALS AND METHODS

RNA 3D structure determination and analysis

RNA2D3D uses constraints obtained from standard A-form helices to obtain a 3D structure by embedding the 3D nucleotides into a planar secondary structure and ultimately winding the structure. The sequence and secondary structure elements of satC, modeled on the structure of the TCV TSS including Ψ_2 and putative Ψ_3, were presented to RNA2D3D to produce initial 3D computational models. Each of the models was subjected to extensive molecular modeling protocols, including manual adjustments and refinements of the structural models followed by mechanics minimization and molecular dynamics equilibrations as previously described (Yingling and Shapiro 2006; Shapiro et al. 2007; Martinez et al. 2008; McCormack et al. 2008).

Construction of TCV mutants

All mutants were constructed using oligonucleotide-mediated site-directed mutagenesis. PCR was conducted using pTCV66 as template, which contains wt TCV sequence downstream of a T7 promoter. All mutants were subjected to regional sequencing to confirm alterations.

Protoplast preparation, inoculation of viral genomic RNA, and RNA gel blots

TCV genomic RNA constructs were digested with SmaI and in vitro transcribed using T7 RNA polymerase. Callus from *Arabidopsis thaliana* ecotype Col-0 was treated with cellulase and pectinase to produce protoplasts that were competent for viral RNA infection as previously described (Zhang et al. 2006b). Twenty micrograms of genomic TCV RNA were inoculated into protoplasts using polyethylene glycol and total RNA extracted at 40 hpi was subjected to electrophoresis, transferred to a nitrocellulose membrane, and the genomic RNA detected using a complementary ^{32}P-labeled oligonucleotide. Blots were stripped

Downloaded from rnajournal.cshlp.org on February 12, 2009 - Published by Cold Spring Harbor Laboratory Press

and then reprobed with a fragment complementary to the ribosomal RNAs. Data was quantified using Quantity One software from BioRad Laboratories, and viral genomic RNA levels were normalized to levels of ribosomal RNA.

Synthesis of RNA fragments used for ribosome binding

Amplification of fragments by PCR used the following primers: for TCV fragment F1, homologous to positions 3901–3912 (all homologous primers except noted included a T7 RNA polymerase promoter for subsequent RNA synthesis) and complementary to positions 3998–4017; F2, homologous to positions 3901–3912 and complementary to positions 4036–4054; F3, homologous to positions 3860–3877 and complementary to positions 3998–4017; F4, homologous to positions 3860–3877 and complementary to positions 4036–4054; FL, homologous to positions 3661–3677 and complementary to positions 4036–4054. For satC fragment CF1, the template was pT7C+ and primers were homologous to positions 206–226 and complementary to positions 304–324. Mutant TCV fragments were generated either using mutant pTCV66 or directly incorporating the mutations into the primers. All PCR products were transcribed using T7 RNA polymerase followed by treatment with RQ1 RNase-free DNase (Promega) to digest the template DNA.

Isolation of 80S ribosomes and 60S/40S ribosomal subunits

Yeast ribosomes (strain JD1090) were isolated as previously described (Meskauskas et al. 2005). Supernates (S30) following cellular disruption were transferred to 4 mL polycarbonate tubes containing either 1 mL of a cushion buffer B (20 mM Tris-HCl at pH 7.5 at 4°C, 5 mM $Mg(CH_3COO)_2$, 0.5 M KCl, 25% glycerol, 1 mg/mL heparin, 1 mM PMSF, 1 mM DTE) (for salt-washed ribosomes), or 1 mL of buffer C (50 mM Tris-HCl at pH 7.5 at 4°C, 5 mM $Mg(CH_3COO2)$, 50 mM NH_4Cl, 25% glycerol, 0.1 mM PMSF, 0.1 mM DTE) (for non-salt-washed ribosomes). Ribosomes were sedimented by centrifugation for 2 h at 50,000 rpm using an MSL-50 rotor. Pellets were gently washed with buffer C, ribosomes suspended in buffer C at concentrations of 2 to 10 pmol/μL (1 OD_{260} = 20 pmol), and then stored frozen at −80°C. For isolation of ribosomal subunits, 80S ribosomes were resuspended in 20 mM HEPES-KOH (pH 7.6), 10 mM $Mg(CH_3COO)_2$, 0.5 M KCl, 1 mg/mL heparin, and 2 mM DTE. Suspensions were loaded onto 10%–30% sucrose gradients in the same buffer and subjected to centrifugation at 20,000 rpm for 16 h at 4°C in an SW41 rotor. Gradients were fractionated and fractions containing 60S and 40S subunits identified by agarose gel electrophoresis. Pooled fractions were dialyzed against 50 mM HEPES-KOH (pH 7.6), 5 mM $Mg(CH_3COO)_2$, 50 mM NH_4Cl, and 2 mM DTE and concentrated on Centricon 100 units (Millipore). Glycerol was then added to a final concentration of 25% and subunits stored at −80°C.

Synthesis of aminoacyl-tRNA and acetylated aminoacyl-tRNA

Yeast phenylalanyl-tRNAs were aminoacylated as previously described (Meskauskas et al. 2005). Phe-tRNA was acetylated in 1 mL of 3 M potassium acetate (pH 5.0) by addition of 64 μL of acetic anhydride at 15-min intervals for 1 h on ice, clarified by centrifugation at 15,000 rpm for 3 min, and purified by HPLC as previously described (Meskauskas et al. 2005).

Ribosome binding assays

Filter binding assays were performed as previously described (Meskauskas et al. 2005) in 50 μL of binding buffer (80 mM Tris-HCl at pH 7.4, 160 mM NH_4Cl, 11 mM $Mg(CH_3COO)_2$, 6 mM β-mercaptoethanol, 0.4 mM GTP, 2 mM spermidine, 0.4 μg/mL of poly(U)] containing 25 pmol of ribosomes and 2–100 pmol of [^{32}P] 5′-end labeled RNA fragments. For $tRNA_{Phe}$ competition experiments, ribosomes (30 pmol) were preincubated with 0–600 pmol of $tRNA_{Phe}$ for 15 min at 30°C (poly[U] was omitted to prevent tRNA binding to the E-site in this assay; Rheinberger et al. 1981). Thirty picomoles of labeled fragment F1 were added and incubations continued for 15 min at 30°C. P-site specificity was determined by incubating 30 pmol ribosomes in binding buffer with 0–600 pmol of F1 for 15 min at 30°C. Subsequently, 30 pmol of Ac-[^{14}C]-Phe-tRNA were added to each reaction, and incubations were continued for 15 min at 30°C. For A-site competition, ribosomes (30 pmol) were preincubated with 120 pmol of tRNA for 10 min at 30°C (to block Phe-tRNA binding to the P-site), then incubated with 0–600 pmol of TCV or satC fragments for 10 min at 30°C, followed by addition of 120 pmol [^{14}C]-Phe-tRNA for 10 min at 30°C. Alternatively, ribosomes were directly incubated with 0–600 pmol of purified F1 followed by addition of [^{14}C]-Phe-tRNA. Data are expressed as percentage of initial binding (without competing RNA) at given competing RNA/ribosomes molar ratios.

Translation assays

The single reporter construct (Fluc) used to assay for translation in vivo contained an upstream segment (30 nt) to which full-length TCV 5′ UTR (positions 1–63) was added. The 3′ end contained a downstream segment (10 nt) to which wt and mutant 3′ region (positions 3661–4054). were added. The 3′C control is a TCV internal fragment (positions 3001–3393) inserted in the minus-sense orientation. Uncapped transcripts (30 μg) synthesized by T7 RNA polymerase were inoculated onto 5×10^6 *Arabidopsis* protoplasts along with 10 μg of uncapped transcripts containing internal control *Renilla* luciferase (Rluc) ORF. Protoplasts were harvested at 18 hpi, cells lysed, and luciferase activity (Promega) measured using a TD 20/20 luminometer (Turner Designs).

ACKNOWLEDGMENTS

This work was supported by grants from the U.S. Public Health Service (GM 061515-05A2/G120CD and GM 61515-01) and the National Science Foundation (MCB-0615154) to A.E.S, the U.S. Public Health Service (GM R0158859 and GM 059958) to J.D.D., and the American Heart Association to A.M. (AHA 0630163N). V.A.S. and J.C.M were supported by NIH Institutional Training Grant T32-AI51967-01. This research was supported in part by the Intramural Research Program of NIH, National Cancer Institute, Center for Cancer Research. The computational support was provided in part by the National Cancer Institute's Advanced Biomedical Computing Center.

Received June 17, 2008; accepted August 20, 2008.

Downloaded from rnajournal.cshlp.org on February 12, 2009 - Published by Cold Spring Harbor Laboratory Press

REFERENCES

Allen, G.S. and Frank, J. 2007. Structural insights on the translation initiation complex: Ghosts of a universal initiation complex. *Mol. Microbiol.* **63:** 941–950.

Baird, S.D., Turcotte, M., Korneluk, R.G., and Holcik, M. 2006. Searching for IRES. *RNA* **12:** 1755–1785.

Barends, S., Bink, H.H., van den Worm, S.H., Pleij, C.W., and Kraal, B. 2003. Entrapping ribosomes for viral translation: tRNA mimicry as a molecular Trojan horse. *Cell* **112:** 123–129.

Bert, A.G., Grépin, R., Vadas, M.A., and Goodall, G.J. 2006. Assessing IRES activity in the HIF-1α and other cellular 5′ UTRs. *RNA* **12:** 1074–1083.

Bradrick, S.S., Walters, R.W., and Gromeier, M. 2006. The hepatitis C virus 3′-untranslated region or a poly(A) tract promote efficient translation subsequent to the initiation phase. *Nucleic Acids Res.* **34:** 1293–1303.

Carpenter, C.D., Oh, J.-W., Zhang, C., and Simon, A.E. 1995. Involvement of a stem-loop structure in the location of junction sites in viral RNA recombination. *J. Mol. Biol.* **245:** 608–622.

Chiu, W.-W., Kinney, R.M., and Dreher, T.W. 2005. Control of translation by the 5′- and 3′ terminal regions of the Dengue virus genome. *J. Virol.* **79:** 8303–8315.

Costantino, D.A., Pfingsten, J.S., Rambo, R.P., and Kieft, J.S. 2008. tRNA-mRNA mimicry drives translation initiation from a viral IRES. *Nat. Struct. Mol. Biol.* **15:** 57–64.

Dobrikova, E.Y., Grisham, R.N., Kaiser, C., Lin, J., and Gromeier, M. 2006. Competitive translation efficiency at the picornavirus type 1 internal ribosome entry site facilitated by viral *cis* and *trans* factors. *J. Virol.* **80:** 3310–3321.

Dreher, T.W. and Miller, W.A. 2006. Translational control in positive strand RNA plant viruses. *Virology* **344:** 185–197.

Fabian, M.R. and White, K.A. 2004. 5′-3′ RNA–RNA interaction facilitates cap- and polyA tail-independent translation of Tomato bushy stunt virus mRNA: A potential common mechanism for Tombusviridae. *J. Biol. Chem.* **279:** 28862–28872.

Fabian, M.R. and White, K.A. 2006. Analysis of a 3′-translation enhancer in a tombusvirus: A dynamic model for RNA–RNA interactions of mRNA termini. *RNA* **12:** 1304–1314.

Fechter, P., Rudinger-Thirion, J., Florentz, C., and Giege, R. 2001. Novel features in the tRNA-like world of plant viral RNAs. *Cell. Mol. Life Sci.* **58:** 1547–1561.

Fraser, C.S. and Doudna, J.A. 2007. Structural and mechanistic insights into hepatitis C viral translation initiation. *Nat. Rev. Microbiol.* **5:** 29–38.

Ganoza, M.C., Kiel, M.C., and Aoki, H. 2002. Evolutionary conservation of reactions in translation. *Microbiol. Mol. Biol. Rev.* **66:** 460–485.

Hacker, D.L., Petty, I.T., Wei, N., and Morris, T.J. 1992. Turnip crinkle virus genes required for RNA replication and virus movement. *Virology* **186:** 1–8.

Hellen, C.U. and Sarnow, P. 2001. Internal ribosome entry sites in eukaryotic mRNA molecules. *Genes & Dev.* **15:** 1593–1612.

Holcik, M. and Sonenberg, N. 2005. Translational control in stress and apoptosis. *Nat. Rev. Mol. Cell Biol.* **6:** 318–327.

Iwakawa, H.O., Kaido, M., Mise, K., and Okuno, T. 2007. *cis*-Acting core RNA elements required for negative-strand RNA synthesis and cap-independent translation are separated in the 3′-untranslated region of Red clover necrotic mosaic virus RNA1. *Virology* **369:** 168–181.

Karetnikov, A., Keränen, M., and Lehto, K. 2006. Role of the RNA2 3′ nontranslated region of Blackcurrant reversion nepovirus in translational regulation. *Virology* **354:** 178–191.

Kneller, E.L., Rakotondrafara, A.M., and Miller, W.A. 2006. Cap-independent translation of plant viral RNAs. *Virus Res.* **119:** 63–75.

Kozak, M. 1999. Initiation of translation in prokaryotes and eukaryotes. *Gene* **234:** 187–208.

Lancaster, A.M., Jan, E., and Sarnow, P. 2006. Initiation factor-independent translation mediated by the hepatitis C virus internal ribosome entry site. *RNA* **12:** 894–902.

Li, W.Z., Qu, F., and Morris, T.J. 1998. Cell-to-cell movement of turnip crinkle virus is controlled by two small open reading frames that function in trans. *Virology* **244:** 405–416.

Marintchev, A. and Wagner, G. 2004. Translation initiation: Structures, mechanisms and evolution. *Q. Rev. Biophys.* **37:** 197–284.

Martinez, H.M., Maizel Jr., J.V., and Shapiro, B.A. 2008. RNA2D3D: A program for generating, viewing and comparing three-dimensional models of RNA. *J. Biomol. Struct. Dyn.* **25:** 669–684.

Matsuda, D. and Dreher, T.W. 2006. Close spacing of AUG initiation codons confers dicistronic character on a eukaryotic mRNA. *RNA* **12:** 1338–1349.

McCormack, J.C. and Simon, A.E. 2004. Biased hypermutagenesis associated with mutations in an untranslated hairpin of an RNA virus. *J. Virol.* **78:** 7813–7817.

McCormack, J.C., Yuan, X., Yingling, Y.G., Zamora, R.E., Shapiro, B.A., and Simon, A.E. 2008. Structural domains within the 3′ UTR of Turnip crinkle virus. *J. Virol.* **82:** 8706–8720.

Merrick, W.C. 2004. Cap-dependent and cap-independent translation in eukaryotic systems. *Gene* **332:** 1–11.

Meskauskas, A., Petrov, A.N., and Dinman, J.D. 2005. Identification of functionally important amino acids of ribosomal protein L3 by saturation mutagenesis. *Mol. Cell. Biol.* **25:** 10863–10874.

Miller, W.A. and White, K.A. 2006. Long-distance RNA–RNA interactions in plant virus gene expression and replication. *Annu. Rev. Phytopathol.* **44:** 447–467.

Miller, W.A., Wang, Z., and Treder, K. 2007. The amazing diversity of cap-independent translation elements in the 3′-untranslated regions of plant viral RNAs. *Biochem. Soc. Trans.* **35:** 1629–1633.

Na, H. and White, K.A. 2006. Structure and prevalence of replication silencer-3′ terminus RNA interactions in *Tombusviridae*. *Virology* **345:** 305–316.

Nagy, P.D., Pogany, J., and Simon, A.E. 1999. RNA elements required for RNA recombination function as replication enhancers in vitro and in vivo in a plus-strand RNA virus. *EMBO J.* **18:** 5653–5665.

Nishimura, K., Sakuma, A., Yamashita, T., Hirokawa, G., Imataka, H., Kashiwagi, K., and Igarashi, K. 2007. Minor contribution of an internal ribosome entry site in the 5′ UTR of ornithine decarboxylase mRNA on its translation. *Biochem. Biophys. Res. Commun.* **364:** 124–130.

Ofengand, J., Gornicki, P., Chakraburtty, K., and Nurse, K. 1982. Functional conservation near the 3′ end of eukaryotic small subunit RNA: Photochemical crosslinking of P site-bound acetyl-valyl-tRNA to 18S RNA of yeast ribosomes. *Proc. Natl. Acad. Sci.* **79:** 2817–2821.

Panaviene, Z., Panavas, T., and Nagy, P.D. 2005. Role of an internal and two 3′-terminal RNA elements in assembly of Tombusvirus replicase. *J. Virol.* **79:** 10608–10618.

Petrov, A., Meskauskas, A., and Dinman, J.D. 2004. Ribosomal protein L3: Influence on ribosome structure and function. *RNA Biol.* **1:** 59–65.

Preiss, T. and Hentze, M.W. 2003. Starting the protein synthesis machine: Eukaryotic translation initiation. *Bioessays* **25:** 1201–1211.

Qu, F. and Morris, T.J. 2000. Cap-independent translational enhancement of Turnip crinkle virus genomic and subgenomic RNAs. *J. Virol.* **74:** 1085–1093.

Rheinberger, H.-J., Sternbach, H., and Nierhaus, K.H. 1981. Three tRNA binding sites on *Escherichia coli* ribosomes. *Proc. Natl. Acad. Sci.* **78:** 5310–5314.

Schilling-Bartetzko, S., Franceschi, F., Sternbach, H., and Nierhaus, K.H. 1992. Apparent association constants of tRNAs for the ribosomal A, P, and E sites. *J. Biol. Chem.* **267:** 4693–4702.

Shapiro, B.A., Yingling, Y.G., Kasprzak, W., and Bindewald, E. 2007. Bridging the gap in RNA structure prediction. *Curr. Opin. Struct. Biol.* **17:** 157–165.

Shen, R. and Miller, W.A. 2004. The 3′ untranslated region of tobacco necrosis virus RNA contains a Barley yellow dwarf virus-like cap-independent translation element. *J. Virol.* **78:** 4655–4664.

Downloaded from rnajournal.cshlp.org on February 12, 2009 - Published by Cold Spring Harbor Laboratory Press

Shen, R. and Miller, W.A. 2007. Structures required for poly(A) tail-independent translation overlap with, but are distinct from, cap-independent translation and RNA replication signals at the 3′ end of Tobacco necrosis virus RNA. *Virology* **358:** 448–458.

Simon, A.E. and Howell, S.H. 1986. The virulent satellite RNA of Turnip crinkle virus has a major domain homologous to the 3′-end of the helper virus genome. *EMBO J.* **5:** 3423–3428.

Song, C. and Simon, A.E. 1995. Requirement of a 3′-terminal stem-loop in in vitro transcription by an RNA-dependent RNA polymerase. *J. Mol. Biol.* **254:** 6–14.

Song, Y., Friebe, P., Tzima, E., Jünemann, C., Bartenschlager, R., and Niepmann, M. 2006. The hepatitis C virus RNA 3′-untranslated region strongly enhances translation directed by the internal ribosome entry site. *J. Virol.* **80:** 11579–11588.

Sun, X. and Simon, A.E. 2006. A *cis*-replication element functions in both orientations to enhance replication of Turnip crinkle virus. *Virology* **352:** 39–51.

Treder, K., Kneller, E.L., Allen, E.M., Wang, Z., Browning, K.S., and Miller, W.A. 2008. The 3′ cap-independent translation element of Barley yellow dwarf virus binds eIF4F via the eIF4G subunit to initiate translation. *RNA* **14:** 134–147.

Triana, F., Nierhaus, K.H., and Chakraburtty, K. 1994. Transfer RNA binding to 80S ribosomes from yeast: Evidence for three sites. *Biochem. Mol. Biol. Interact.* **33:** 909–915.

Ulbrich, B., Mertens, G., and Nierhaus, K.H. 1978. Cooperative binding of 3′ fragments of transfer ribonucleic acid to the peptidyltransferase centre of *Escherichia coli* ribosomes. *Arch. Biochem. Biophys.* **190:** 149–154.

Van Noort, J.M., Kraal, B., and Bosch, L. 1985. A second tRNA binding site on elongation factor Tu is induced while the factor is bound to the ribosome. *Proc. Natl. Acad. Sci.* **82:** 3212–3216.

Wells, S.E., Hillner, P.E., Vale, R.D., and Sachs, A.B. 1998. Circularization of mRNA by eukaryotic translation initiation factors. *Mol. Cell* **2:** 135–140.

Wilson, J.E., Pestova, T.V., Hellen, C.U., and Sarnow, P. 2000. Initiation of protein synthesis from the A site of the ribosome. *Cell* **102:** 511–520.

Wu, B. and White, K.A. 1999. A primary determinant of cap-independent translation is located in the 3′-proximal region of the Tomato bushy stunt virus genome. *J. Virol.* **73:** 8982–8988.

Yingling, Y.G. and Shapiro, B.A. 2006. The prediction of the wild-type telomerase RNA pseudoknot structure and the pivotal role of the bulge in its formation. *J. Mol. Graph. Model.* **25:** 261–274.

Yoshii, M., Nishikiori, M., Tomita, K., Yoshioka, N., Kozuka, R., Naito, S., and Ishikawa, M. 2004. The *Arabidopsis* cumumovirus multiplication 1 and 2 loci encode translation initiation factors 4E and 4G. *J. Virol.* **78:** 6102–6111.

Zhang, J. and Simon, A.E. 2005. Importance of sequence and structural elements within a viral replication repressor. *Virology* **333:** 301–315.

Zhang, J., Stuntz, R.M., and Simon, A.E. 2004. Analysis of a viral replication repressor: Sequence requirements for a large symmetrical internal loop. *Virology* **326:** 90–102.

Zhang, G., Zhang, J., George, A.T., Baumstark, T., and Simon, A.E. 2006a. Conformational changes involved in initiation of minus-strand synthesis of a virus-associated RNA. *RNA* **12:** 147–162.

Zhang, J., Zhang, G., Guo, R., Shapiro, B.A., and Simon, A.E. 2006b. A pseudoknot in a preactive form of a viral RNA is part of a structural switch activating minus-strand synthesis. *J. Virol.* **80:** 9181–9191.

Zhang, J., Zhang, G., McCormack, J.C., and Simon, A.E. 2006c. Evolution of virus-derived sequences for high level replication of a subviral RNA. *Virology* **351:** 476–488.